ACS OMEGA

http://pubs.acs.org/journal/acsodf

Article

# Quantification of Peptide-Bound Particles: A Phage Mimicking Approach via Site-Selective Immobilization on Glass

Martin Schrader,* Caroline Bobeth, and Franziska L. Lederer

Cite This: *ACS Omega* 2022, 7, 187−197

Read Online

ACCESS | Metrics & More | Article Recommendations | Supporting Information

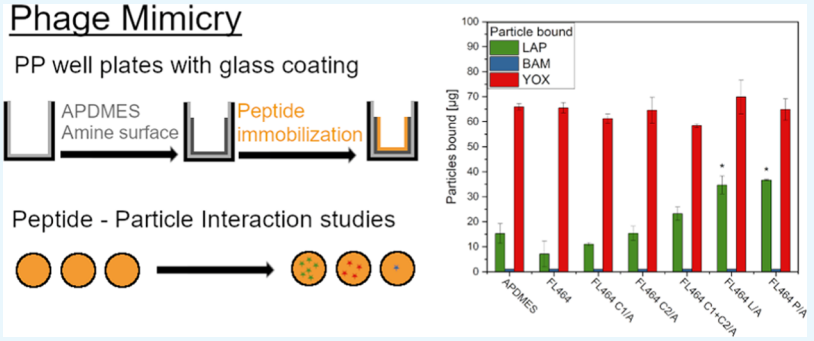


**ABSTRACT:** The increasing complexity and need of high-tech materials for modern electronics raise the demand for rare earth elements. While recycling rates are still negligible for most elements, geopolitical tensions, circular economy, and the aim for a carbon-neutral society put pressure on conventional supply strategies and emphasize the need for new ideas for recycling. Our research group works on the development of phage surface display (PSD)-derived peptide-based recycling methods for electronic waste. This study focuses on $LaPO_4$:Ce,Tb (LAP), a component of electronic waste from compact energy-saving lamps containing rare earth element-enriched fluorescent powders. While free solution-phase peptides show little to no interaction with the target material, we re-enabled the binding capability by immobilizing them on various glass supports. We shine a spotlight on the transition from phage-bound to free peptides and present the first proof of successful peptide-LAP particle interactions of previously reported PSD-derived sequences. Therefore, we introduce a method to investigate peptide−particle−interactions qualitatively and quantitatively. Additionally, a calibration curve allowed the quantification of peptide-bound particles. Combined with the quantification of the immobilized peptide on the surface, it was possible to calculate a potential dosage of peptides for future recycling processes.

## 1. INTRODUCTION

The rising demand for high-tech materials, electronics, and consumables has led to an increasing need for rare earth elements (REE). Furthermore, the challenging composition of modern high-tech products fuels the need for novel recycling techniques and highlights the limitation of traditional methods.[1] Similarities in the chemical properties of these elements make the extraction, separation, and purification challenging and expensive.[2] This is particularly true for end-of-life products, which often contain an even more complex composition and structure as primary resources. The global aim to reduce carbon emissions and environmental impact, as well as geopolitical tensions put pressure on conventional mining and trading strategies. Those factors underline the importance of developing novel, beneficial, and greener recycling techniques. One promising secondary resource for REE is a fluorescent lamp powder (FLP) from compact energy-saving lamps (CESL). While the phosphor powders only add up to around 3 wt % of CESL, the contained REE represents around 32% of the global market share in terms of value.[3,4] The amount of REE bound in lamp phosphors is expected to be around 25 000 tons for the year 2020, while end-of-life products will take a share of up to 4200 tons. The mainly used phosphors are $Y_2O_3$:Eu (YOX), $LaPO_4$:Ce,Tb (LAP), $CeMgAl_{11}O_{19}$:Tb (CAT), and $BaMgAl_{10}O_{17}$:Eu (BAM), with especially YOX and LAP containing high ratios of REE.[4] While YOX can be selectively recycled already, the separation of the other components is still challenging.[5]

The approach of the research group BioKollekt aims for the development of modern peptide-based recycling techniques for critical raw materials in electronic waste and starts with REE-containing FLP as a proof of principle. This approach focuses

Received: August 12, 2021
Accepted: November 29, 2021
Published: December 20, 2021

on the development of biohybrid materials for the selective binding and finally separation of target materials from a complex material mixture. The first step to achieve this vision was done during the project MinePep with the identification of peptides that are specific for REE-containing FLP components. Phage surface display (PSD) technology on particles sized 1−10 $\mu$m was performed in the beginning using YOX. Due to toxic leaching effects of YOX, LAP and CAT were chosen as new target materials. In individual PSD procedures and while using three different pVIII phage peptide libraries, a few peptides that are highly specific for the fluorescent phosphors LAP and CAT were identified.[6−8] In the following approach, one of the identified peptides specific for LAP, RCQYPLCS (alias FL464), was expressed in modified forms using alanine scanning mutagenesis. Each amino acid in that peptide was replaced by an alanine. The phages with modified peptide composition were analyzed in individual target binding studies.[6] Phages tend to mutate within a very short time due to missing proofreading mechanisms during replication. Within a few phage amplification cycles, the number of phages that miss the target-specific peptides increased while the number of those phages that express the additional peptides decreased.[9] These findings rule out the application of phages in the aimed recycling process. Due to this limitation, the successfully identified peptide motives that are specific for LAP and CAT were tested in a subsequent approach without phage.

For the transitioning, the peptides identified via PSD were synthesized chemically and tested on their binding behavior again. However, this transitioning from phage-bound peptides to chemically synthesized peptides in solution proved challenging due to the fact that most analytics are developed for solution-phase chemistry, show problems with fast settling particles, or are not suitable for the intended concentration range. In preliminary tests, the peptides were brought into direct contact with the target material LAP (unpublished data). First interaction studies were carried out via UV−vis measurements, but no reliable proof of interaction was detectable. Furthermore, HPLC, ATR-IR, and NMR experiments were performed without yielding a proof beyond any doubt.

The aforementioned struggles lead us to new methodological approaches. Mimicking the phage surface could overcome the mentioned hurdles and either re-enable the binding capabilities of the peptides or re-enable the investigation of the interactions via standard laboratory equipment.

In the following study, a convenient method for testing and comparing particle binding peptides by immobilizing them on glass supports is presented, using commercial microscopic slides as well as self-modified microscopic slides and glass-coated 96-well microplates (MTP). Quantification was performed via fluorescence scanning in a plate reader, taking into account the inhomogeneity of particles and exploiting the fluorescence properties of the target material.

This study states the first proof of concept for PSD-derived peptide-induced adhesion for the development of peptide-based recycling techniques for REE-containing FLP.

## 2. RESULTS

**2.1. Qualitative Binding Tests.** To gain knowledge about interaction and differences, a quick screening on commercial diagnostic microscopic slides was performed. Those slides have a poly(tetrafluoroethylene) (PTFE) mask with only 12 spots per slide being functionalized glass. The peptides therefore were only immobilized on the unmasked coated glass spots. Two spots per slide were left as negative controls as untreated glass (Figure 1, spot 1) and as treated with the coupling agent mixture (Figure 1, spot 2).

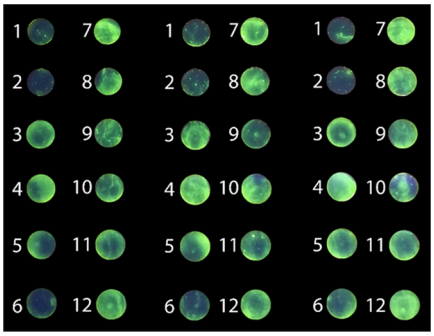


**Figure 1.** Binding test of LAP with 5 $\mu$L (100 $\mu$g, 77 nmol) peptide immobilized with a 2.5 $\mu$L solution of PyBOP (1.2 equiv, 19 mg in 1 mL) and DiPEA (3 equiv, 10.5 $\mu$L) in NMP per spot on commercial silanized and PTFE-masked diagnostic slides. PTFE mask was blacked for better visibility. The fluorescence, $\lambda_{ex}$: 254 nm via a UV lamp, shows differences in the binding behavior of the peptides toward the target material. Legend: 1: untreated; 2: treated with PyBOP; 3: FL464 S/A; 4: FL464 R/A; 5: FL464 Y/A; 6: FL464 Q/A; 7: FL464; 8: FL464 C1/A; 9: FL464 C2/A; 10: FL464 C1+C2/A; 11: FL464 L/A; 12: FL464 P/A.

As seen in Figure 2, there is a significant amount of LAP adhered on the spots where peptides were immobilized, while

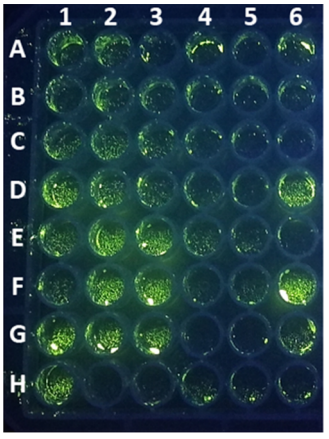


**Figure 2.** Glass-coated well plates with APDMES coating and 100 $\mu$g immobilized peptides. Image of the well plate with adhered LAP on immobilized peptides, $\lambda_{ex}$: 254 nm via UV lamp. Well assignments: A1-3 Glass; B1-3 APDMES; C1-3 FL464 C1+C2/A; D1-3 FL464 C1/A; E1-3 FL464 C2/A; F1-3 FL464 L/A; G1-3 FL464 P/A; H1-3 FL464 Q/A; A4-6 FL464 R/A; B4-6 FL464 S/A; C4-6 FL464 Y/A; D4-6 FL464.

on the negative controls 1 and 2, only a small amount of powder is bound. Especially FL464 (Figure 1, spot 7) and FL464 P/A (Figure 1, spot 12) seem outstanding, while FL464 Q/A (Figure 1, spot 6) adhered the least amount of LAP of the peptides.

**2.2. Fast Semiquantitative Screening for Peptides.** To develop a quantifiable approach for comparison of the peptides, glass-coated microplates were used. The previously


https://doi.org/10.1021/acsomega.1c04343
ACS Omega 2022, 7, 187−197

tested amine functionalization via silanization with APDMES was chosen.

An image of the result of the binding test is shown in Figure 2, revealing differences between the peptides already.

For further comparison, the fluorescence signal of each pixel measured via fluorescence scanning was summed up. The median of the triplicates is normalized against the APDMES fluorescence sums as blank, resulting in relative fluorescence. As seen in Figure 3 and Table 1, the peptides FL464 C2/A and

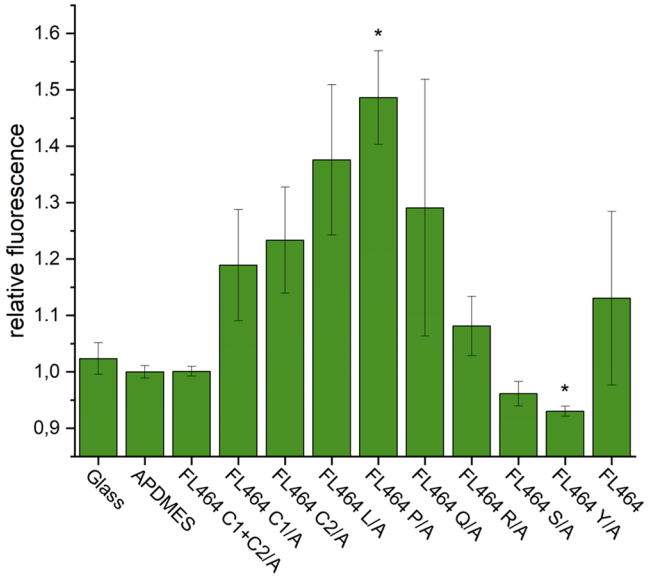


**Figure 3.** Results of quantitative screening of immobilized peptides adhered LAP. Sums of the fluorescence ($\lambda_{ex}$: 365 nm, $\lambda_{em}$: 550 nm) scanning were referenced on APDMES as blank. Error bars represent the REM; the star above a bar highlights significance with $P$ value <.05. The $P$ values for the significant results are .02 and .007 for FL464 P/A and FL464 Y/A, respectively.

FL464 C1/A showed strong adhesion with especially FL464 L/A with 1.38 ± 0.15% and FL464 P/A showing the most adhesion from up to 1.49 ± 10% relative to the blank. FL464 Q/A showed high values as well, but on visual evaluation of the MTP, only one well showed noticeable adhesion, thus also leading to a high REM. The same applies for FL464, although the variation is lower.

Calculating the $P$ values showed that the peptides, FL464 C2/A, FL464 L/A, and FL464 P/A and FL464 Y/A achieved values <.12, with only FL464 P/A achieving a value <.05 (with $P$ = .02) for adhering more LAP and FL464 Y/A ($P$ = .007) for adhering significant less LAP than the blank and therefore being marked as significant in Figure 3 with an $\alpha$ of .05.

**2.3. Equimolar Quantitative Screening for Peptides with Calibration Curve.** Due to different molar weights, see Table 6, we performed another set of experiments with equimolar peptide concentrations, thus yielding more comparable results on a molecular basis. Contrary to the prior experiment, the well plate was washed three consecutive times, which highly reduced the standard deviation within the triplicate and yielding a low REM of ≤2% (see Table 2). After washing, the calibration curve experiment was prepared on the same plate. The analysis of the data is done accordingly, and the results of the summed fluorescences are shown in Figure 4, as well as Table 2, which also contains the relative fluorescence normalized on FL464 for each respective concentration and the amount of the bound LAP. Figure 5 shows the calibration curve. Figure 6 shows the calculated peptide-bound amount of LAP (Table 2).

These results in general show a similar trend, with the peptides containing just one thiol group (FL464 C1/A and FL464 C2/A) showing less adhesion compared to the prior experiment. As shown in Figure 5, the fluorescence does not increase linearly in low concentrations but in a quadratic curve for the used concentration range. With this concentration curve, the amount of bound powder can be calculated, as shown in Figure 6 and Table 2. Although the relative fluorescence suggests differences from up to 25% (FL464 to FL464 P/A in 1.43 mM), the actual amount of bound powder differs from 11.13 to 43.70 $\mu$g, which equals an increase of a factor of 393% for the same comparison.

Furthermore, the only significant ($\alpha$ = .05) change in adsorption due to concentration is for FL464 P/A from 0.48 to 1.43 mmol with $P$ = .001, which corresponds to an increase of 16% of bound LAP for the tripled amount of peptide.

**2.4. Quantification of Peptides on Surface and Dosage Calculation.** UV−vis adsorption measurements on a freshly coated and peptide-bearing MTP plate enabled the quantification of peptide immobilized on the surface.

In general, the amount of peptide immobilized was rather constant for each peptide within the three used concentrations. However, in the peptides FL464 (17%) and FL464 C1/A (36%), a significant increase ($P$ > .01) from the lowest to highest concentration was observed. FL464 P/A and FL464 L/A showed rather low immobilization rates compared to the other peptides with up to 6 times less peptide immobilized compared to FL464.

These data, together with the results of Section 2.3, allows also the estimation of potential dosages and potentially bound lap per mol of peptide for future applications and recycling processes.

Figure 7 shows the estimated amount of LAP that can be bound by 1 mol of peptide for the peptides, combined for all concentrations used each, with FL464 L/A and FL464 P/A

**Table 1. Results of the Semiquantitative Screening for Peptides**[a]

| peptide | rel. fluo. | REM in % | $P$ | peptide | rel. fluo. | REM in % | $P$ |
|---|---|---|---|---|---|---|---|
| glass | 1.02 ± 0.03 | 2.81 | | FL464 P/A | 1.49 ± 0.12 | 8.30 | .02 |
| APDMES | 1.00 ± 0.01 | 1.11 | | FL464 Q/A | 1.29 ± 0.29 | 22.8 | .38 |
| FL464 C1+C2/A | 1.00 ± 0.01 | 0.87 | .95 | FL464 R/A | 1.08 ± 0.06 | 5.23 | .23 |
| FL464 C1/A | 1.19 ± 0.12 | 9.86 | .18 | FL464 S/A | 0.96 ± 0.02 | 2.18 | .18 |
| FL464 C2/A | 1.23 ± 0.12 | 9.41 | .12 | FL464 Y/A | 0.93 ± 0.01 | 0.89 | .007 |
| FL464 L/A | 1.38 ± 0.18 | 13.3 | .11 | FL464 | 1.13 ± 0.17 | 15.4 | .50 |

[a]rel. fluo. = relative fluorescence.



https://doi.org/10.1021/acsomega.1c04343
ACS Omega 2022, 7, 187−197

Table 2. Results of the Equimolar Quantitative Screening[a]

| peptide | $c$ [mM] | sum. fluo. [au] | REM [%] | rel. fluo. | $P$ | LAP [$\mu$g] | REM [%] | $P$ |
|---|---|---|---|---|---|---|---|---|
| FL464 | 0.48 | 40 475 | 1.28 | 1.00 ± 0.01 | | 10.33 | 28.06 | |
| | 0.96 | 41 541 | 2.07 | 1.00 ± 0.02 | | 7.14 | 72.20 | |
| | 1.43 | 40 600 | 1.03 | 1.00 ± 0.01 | | 11.13 | 20.03 | |
| FL464 | 0.48 | 40 016 | 1.24 | 0.99 ± 0.01 | .56 | 7.74 | 37.38 | .56 |
| C1/A | 0.96 | 40 051 | 0.31 | 1.01 ± 0.00 | .59 | 11.01 | 5.96 | .50 |
| | 1.43 | 40 803 | 0.72 | 1.01 ± 0.01 | .72 | 12.26 | 12.21 | .69 |
| FL464 | 0.48 | 43 181 | 1.29 | 1.07 ± 0.01 | .02 | 22.26 | 9.04 | .03 |
| C2/A | 0.96 | 40 544 | 1.59 | 1.04 ± 0.02 | .24 | 15.35 | 18.46 | .24 |
| | 1.43 | 43 325 | 0.55 | 1.07 ± 0.01 | .005 | 22.87 | 3.67 | .008 |
| FL464 | 0.48 | 42 616 | 1.23 | 1.05 ± 0.01 | .04 | 20.12 | 10.4 | .052 |
| C1+C2/A | 0.96 | 41 499 | 1.72 | 1.09 ± 0.02 | .04 | 23.25 | 11.72 | .051 |
| | 1.43 | 44 696 | 1.44 | 1.10 ± 0.02 | .006 | 27.44 | 7.67 | .006 |
| FL464 | 0.48 | 45 152 | 1.09 | 1.12 ± 0.01 | .003 | 28.93 | 5.20 | .005 |
| L/A | 0.96 | 43 480 | 2.69 | 1.18 ± 0.03 | .009 | 34.70 | 10.36 | .01 |
| | 1.43 | 46 965 | 1.87 | 1.16 ± 0.02 | .003 | 34.18 | 6.99 | .002 |
| FL464 | 0.48 | 48 213 | 0.55 | 1.19 ± 0.01 | <.001 | 37.63 | 1.83 | <.001 |
| P/A | 0.96 | 47 205 | 0.25 | 1.20 ± 0.00 | <.001 | 36.68 | 0.85 | .005 |
| | 1.43 | 50 680 | 0.28 | 1.25 ± 0.00 | <.001 | 43.70 | 0.77 | <.001 |

[a]sum. fluo. = summed fluorescence; rel. fluo. = relative fluorescence normed on FL464 in the respective concentration.

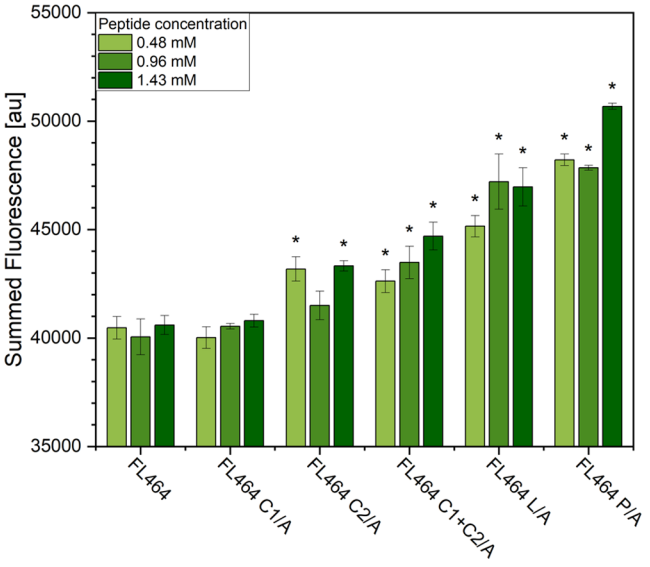


Figure 4. Results of equimolar concentration screening of immobilized peptides adhering LAP. Sums of the fluorescence ($\lambda_{ex}$: 365 nm, $\lambda_{em}$: 550 nm) scanning are shown. Error bars represent the SE; the star above a bar highlights a $P$ value <.05. The $P$ values for the significant results are listed in Table 3.

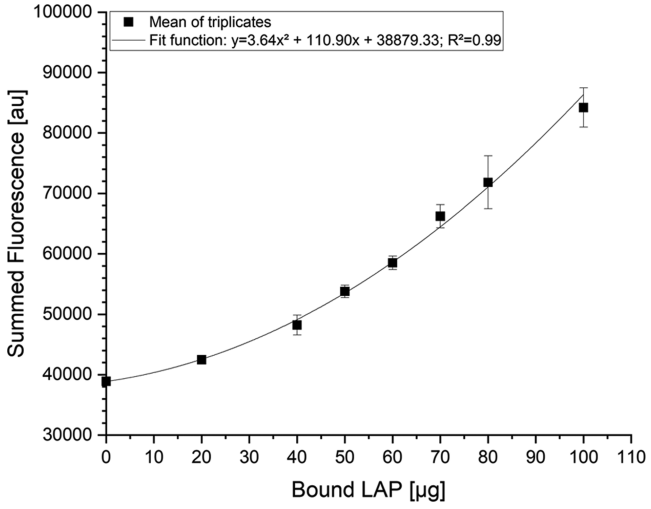


Figure 5. Calibration curve with summed fluorescence in the range of 0−100 $\mu$g. The equation of the quadratic fit function is $y = 3.64x^2 + 110.90x + 38879.34$ with an $R^2$ of 0.99.

showing both very high binding potential compared to the other peptides.

**2.5. Selectivity Testing.** To compare the adhesion characteristics of the peptides for the other main phosphors of CESLs, the procedure of Section 2.3 was repeated for YOX and BAM. These particles feature different excitation and emission wavelengths that renders a comparison via the fluorescence signal meaningless. Instead, a calibration curve for each compound was measured and the amount of bound powder was calculated. Peptides were immobilized in glass wells, while another plate was prepared containing the calibration curves.

The results furthermore were tested on significance ($P$ < .05) for an increase/decrease of adhesion compared to the coating itself. The results are shown in Figure 8 and Table 4.

In general, YOX adhered in relatively high amounts through all samples without any significant difference. For BAM, FL464 P/A showed significantly less adhesion compared to the APDMES coating ($P$ = .007). However, BAM is barely bound, ranging from 1.04 to 1.10 $\mu$g for all samples.

For both YOX and BAM, no significant change for enhanced adhesion was registered, hinting at a rather unspecific binding between the surfaces and particles.

For LAP, although the results are not significant, it is noteworthy that FL464 adhered less particles than the coating itself, indicating a different binding mechanism. However, there is a significant increase of adhered LAP observed for the peptides FL464 L/A ($P$ = .02) and FL464 P/A ($P$ = .005) compared to the APDMES. The relatively large change in adhesion depending on peptide structure indicates a more specific interaction. Therefore, only selectivity of the peptides toward LAP was observable.


https://doi.org/10.1021/acsomega.1c04343
ACS Omega 2022, 7, 187−197

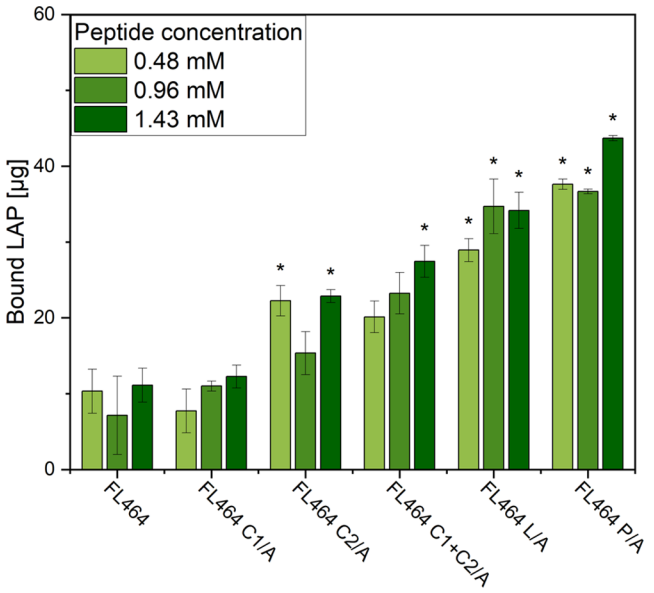


**Figure 6.** Calculated amount of peptide-bound LAP powder (in $\mu$g) of the equimolar concentration screening of immobilized peptides. Error bars represent the SE; the star above a bar highlights a $P$ value <.05 for the change referenced to FL464. The $P$ values for the significant results are listed in Table 2.

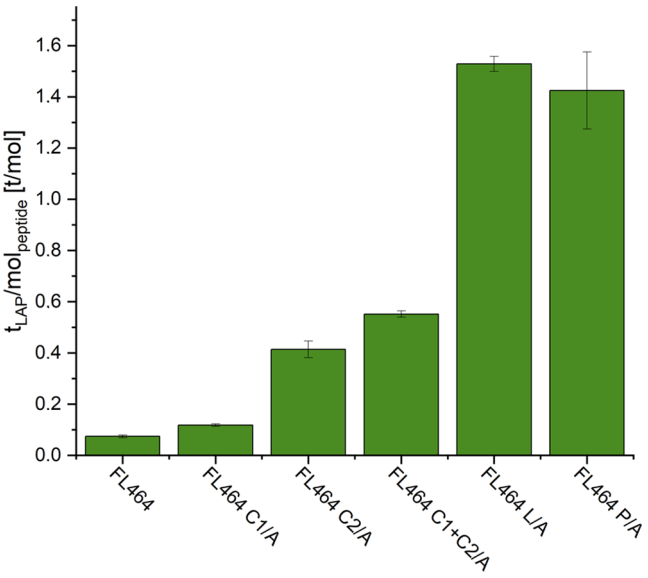


**Figure 7.** Binding capacity of the peptides in tons of LAP per mol of peptide of the investigated peptides.

**2.6. MM2 Simulation.** Energy minimization calculations yielded a potential structure of the respective peptides in a local energy minimum. Example pictures of the calculated potential structures of FL464 and FL464 P/A are shown in Figure 9. Further pictures of other peptides are in the Supporting Information (Figure S1). Considering that the immobilization is performed on the C-terminus, it is notable that FL464 P/A is the only peptide, of the six further investigated, where the C-terminus and N-terminus ended in a close distance, while in all other peptides, the C-terminus and N-terminus tend to be in opposite directions of the molecule. Furthermore, FL464 P/A and FL464 L/A display a hydrophobic backbone on the other side of the C-terminus, while all other peptides display more polar functionalities.

## 3. DISCUSSION

Specific binding peptides bear a great potential as surface-modifying molecules, enabling the development of novel recycling technologies. In previous work, we identified peptides selectively binding on REE-containing fluorescent lamp powder particles. With the new experiments outlined above, we are able to show the first proof of an interaction of the PSD-derived peptides from Lederer et al.[6] In previous preliminary experiments, this showed to be troublesome. First, interaction studies were carried out via UV−vis measurements. LAP in 10- to 1000-fold excess was treated with various identified peptides in six different buffer solutions

**Table 3. Calculated Immobilized Peptide for the Respective Concentrations**[a]

| peptide | concentration used [mM] | immobilized peptide [pmol] | REM [%] | estimated dosage [$g_{peptide}/t_{LAP}$] | LAP per mol [$t_{LAP}/mol_{peptide}$] |
|---|---|---|---|---|---|
| FL464 | 0.48 | 119.1 | 13.2 | 11 149 | 0.09 |
| | 0.96 | 127.2 | 11.6 | 17 225 | 0.06 |
| | 1.43 | 138.9 | 8.0 | 12 070 | 0.08 |
| FL464 | 0.48 | 75.2 | 6.3 | 9104 | 0.10 |
| C1/A | 0.96 | 83.4 | 10.5 | 7102 | 0.13 |
| | 1.43 | 102.6 | 9.7 | 7839 | 0.12 |
| FL464 | 0.48 | 45.5 | 14.8 | 1916 | 0.49 |
| C2/A | 0.96 | 50.9 | 22.5 | 3108 | 0.30 |
| | 1.43 | 50.7 | 9.4 | 2077 | 0.45 |
| FL464 | 0.48 | 37.2 | 13.4 | 1672 | 0.54 |
| C1+C2/A | 0.96 | 39.2 | 13.3 | 1526 | 0.59 |
| | 1.43 | 52.7 | 36.3 | 1737 | 0.52 |
| FL464 | 0.48 | 18.9 | 28.3 | 604 | 1.53 |
| L/A | 0.96 | 24.1 | 8.5 | 643 | 1.44 |
| | 1.43 | 21.2 | 26.6 | 572 | 1.62 |
| FL464 | 0.48 | 35.1 | 59.7 | 878 | 1.07 |
| P/A | 0.96 | 19.0 | 34.0 | 487 | 1.93 |
| | 1.43 | 34.5 | 47.3 | 743 | 1.27 |

[a]Quantification via UV−vis measurements ($\lambda$: 280 nm). For dosage calculation (less = better) and calculation of LAP per mol of peptide (more = better), the obtained amount of peptide was set in relation to the amount of LAP bound in Section 2.3.



https://doi.org/10.1021/acsomega.1c04343
ACS Omega 2022, 7, 187−197

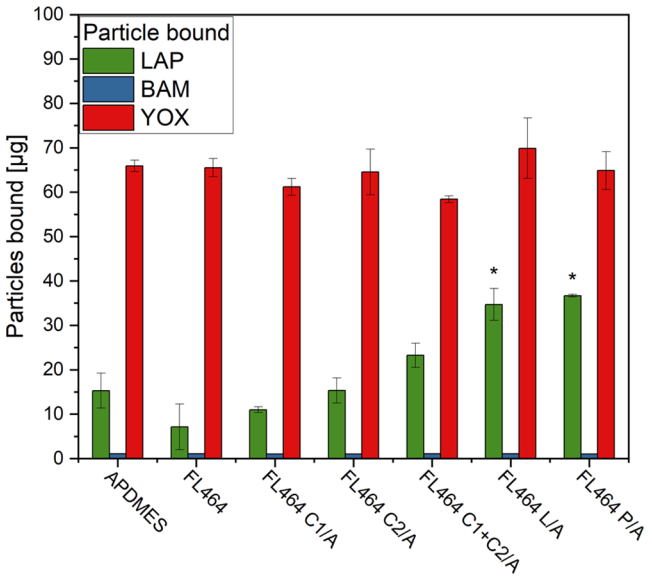


**Figure 8.** Comparison of the amount of bound lamp powder for the different peptides and particles. Error bars represent the SE; the star above a bar highlights a $P$ value <.05 for the change referenced to APDMES. The $P$ values for the significant results for LAP are .02 (FL464 L/A, more adhesion) and .005 (FL464 P/A, more adhesion) and .007 for BAM (FL464 P/A, less adhesion).

**Table 4. Calculated Amount of Adhered Lamp Powder for Different Phosphors (in $\mu$g) for the Selectivity Test**

| peptide | bound amount of LAP [$\mu$g] | bound amount of YOX [$\mu$g] | bound amount of BAM [$\mu$g] |
|---|---|---|---|
| APDMES | 150.3 ± 3.9 | 65.9 ± 1.3 | 1.10 ± 0.0 |
| FL464 | 7.14 ± 5.2 | 65.5 ± 2.1 | 1.08 ± 0.0 |
| FL464 C1/A | 11.1 ± 0.7 | 64.5 ± 5.2 | 1.05 ± 0.0 |
| FL464 C2/A | 15.4 ± 2.8 | 58.4 ± 0.8 | 1.05 ± 0.0 |
| FL464 C1+C2/A | 23.3 ± 2.7 | 61.2 ± 1.9 | 1.07 ± 0.0 |
| FL464 L/A | 34.7 ± 3.6 | 69.9 ± 6.8 | 1.08 ± 0.0 |
| FL464 P/A | 36.7 ± 0.3 | 64.9 ± 4.3 | 1.04 ± 0.0 |

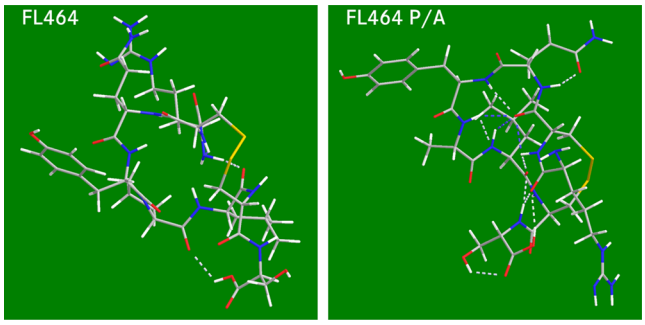


**Figure 9.** Pictures of the result of energy minimization calculations using an MM2 forcefield showing a potential conformation of the peptides in a local energy minimum. Left: FL464 (sequence: RCQYPLCS); right: FL464 P/A (sequence: RCQYALCS).

with varied pH with and without additives like Tween 20 or tris(hydroxymethyl)-aminomethane (Tris). After an incubation time, the supernatant was measured via UV−vis spectroscopy as well as HPLC. Although we were able to calculate potential bound peptides, the reproducibility and the influence of the buffer solutions showed to be problematic. In another experiment, ATR-IR measurements were performed. An immobilized film of LAP was overflown with a peptide solution. No changes in the spectra or peak form were noticeable and thus no interaction was provable. First NMR experiments showed problematic due to the fast settling of the LAP particles. However, the observed intense peak broadening and changes in the chemical shifts hint at interactions taking place. Nevertheless, they can also be misleading and hard to interpret due to the inhomogeneity in the magnetic field caused by the REE-containing and magnetic particles, thus needing further investigations. Those hurdles lead us to the consideration that the transition from phage-bound to solution-phase free peptides might be troublesome. To overcome these barriers, we decided to develop a phage mimicking approach and demonstrate its success in the present work.

The introduced method uses a set of chemical reactions for the coating as well as for the immobilization to overcome these possible issues by mimicking the phage surface. This was achieved by attaching the C-terminus to the amine-bearing surface—as they are on phage. Immobilization also enables multiple binding sites per particle toward the peptide-bearing surface, thus enabling stronger overall interactions. This approach offers great and needed flexibility when working with particles or various analytical machines due to the high variability in the geometry of the samples. The method is also adjustable to work with nonfluorescent targets using luminescence, absorption, or transmission scanning techniques of modern plate readers. Peptide interactions with organic molecules as targets could be investigated by fluorescence labeling of the target, different UV−vis absorption, or by changes in the contact angle.

The newly introduced method also has its limitations. APDMES is less prone to forming multilayers compared to other aminoalkylsilanes and is known to reliably form self-assembling monolayers on glass surfaces. The coating process itself, however, is still sensitive to moisture, reaction time, used solvents, and reaction temperature, thus resulting in multilayers or defects in the quality due to loosely bound physisorption. This, due to the amine and silanol as functional polar groups present, offers various interaction possibilities with the target materials themselves. Also, the coating is not completely inert to hydrolysis but can withstand short times in aqueous solutions.[10] It is noteworthy that, during the experiments, no loss of adhered particles or functionality even after excessive washing, treating with up to 6 M KOH or concentrated hydrochloric acid solutions, nor organic solvents as elution methods was observable. The adhesion of LAP particles even withstands physical shear forces such as wiping with a tissue.

Another limitation is the used immobilization technique itself as it offers only limited control neither on the amount of peptide bound nor on the formation of peptide polymers—which both varies naturally depending on the peptides used. This could be overcome with the use of selective methods that bind specifically on N- or a modified C-terminus that would request additional chemical treatment of both coating and peptide. Another possibility would be the use of protection-group chemistry. This exact same problem however holds also true for future potential usage of immobilized peptides, thus highlighting the used method as a system with good practical comparability.

Such a mimicking approach started with the use of microscopic slides for a first qualitative screening, which enables quick testing of various peptide sequences and an


https://doi.org/10.1021/acsomega.1c04343
ACS Omega 2022, 7, 187−197

empirical quantitative screening (see Supporting Information). While the commercially available precoated slides provide a more reliable coating, the use of self-modified slides enables quick tests at very low costs. Most of the chemicals are readily available in biological or chemistry working labs with no special equipment needed. Although the target material binds unspecific to glass as well as the coating itself, it is possible to visualize differences in the binding affinity of the various peptides.

The first semiquantitative screening revealed that the peptides FL464 L/A and P/A performed the best, followed by the linear peptides with substituted cysteines FL464 C1/A, FL464 C2/A, and FL464 C1+C2/A. A similar trend within those five peptides is further visible in the second MTP experiment (Section 2.3), although the linear peptides FL464 C1/A and FL464 C2/A performed worse than FL464 C1+C2/A. The substitution of one or more cysteines prevents intramolecular cysteine cyclization and raises flexibility in the structure. Leucine, proline, and, partly, tyrosine are the only apolar amino acids present in the structure of the FL464 peptide series. However, since they get substituted against alanine, another apolar amino acid, the reduction of the hydrophobicity is not the only factor to be considered. Proline, due to its unique structure, is known for breaking secondary and tertiary structures and introducing high conformational rigidity. Since alanine is sterically less demanding than both proline and leucine, the functional groups of the other amino acids could be more accessible and available for binding the target material. A special interest comes to tyrosine. The semiquantitative binding resulted in FL464 Y/A, where tyrosine is substituted against alanine, being significantly worse than the coating and all other peptides. Thus, the substitution of tyrosine leads to a significant reduction of bound LAP and a loss of affinity.

In the conformations yielded from the energy minimization calculations, it is notable that FL464 P/A is the only peptide from the six investigated that has both C- and N-terminus on one side and in close distance to each other. This would hinder immobilization due to steric hindrance and also results in an apolar backbone displayed to the outside with especially tyrosine prominently presented. A similar backbone is displayed in FL464 L/A (Figure S1). Furthermore, the likeliness to form intramolecular hydrogen bonds varies substantially between the peptides. However, the yielded conformation of FL464 only forms two hydrogen bonds, FL464 P/A forms 11 and FL464 L/A 10, hinting at a much more rigid structure.

The measured and calculated amount of peptide immobilized showed that roughly up to 6 times as much FL464 and FL464 C1/A is immobilized compared to FL464 L/A and FL464 P/A and 2 times higher than all other peptides. Additionally, only FL464 and FL464 C1/A showed a significant addition of peptide on the surface from the lowest to highest concentration. However, a similar range of concentrations of the peptide on the surface for the other peptides suggests a saturation of the surface even in the lowest concentrations and the susceptibility to form multilayers for FL464 and FL464 C1/A.

However, one needs to be aware that the plate is measured dry while the extinction coefficients were measured in aqueous media; thus, the extinction coefficient can vary. Since the peptides have similar extinction coefficients and similar sequences, it is assumed that they would behave similarly if the solvent is removed. In our setup, 0.48 mM concentrations proved to be sufficient to ensure reliable data collection.

Overall, the concentration showed to have no strong influence on immobilized peptides or the binding of LAP. In Section 2.3, the only significant change in bound powder was for FL464 P/A going from the lowest to highest concentration. About 16% more powder was bound, while the amount of peptide used tripled. This supports the assumption of saturated surfaces.

Compared to the findings of the PSD, the results of this study differ quite a lot, as seen in Table 5. The biggest change in affinity is notable with FL464 C1/A, which performed, each compared to FL464, 46 times worse in this type of experiment than during the PSD. FL464 L/A instead performed 6 times better during this set of experiments, while the other two (FL464 P/A and FL464 C2/A) performed rather similarly to the PSD. Contrary to those differences in binding affinity, the immobilized peptides showed similar selectivity and rather specific binding for LAP while generally showing no significant adhesion against the other phosphors YOX and BAM compared to APDMES as coating, hinting at a rather unspecific binding for the red and blue phosphor.

**Table 5. Comparison of the Binding Affinity Data from PSD[6] vs Equimolar Quantitative Screening for Peptides with Calibration Curve among the 1.43 mM Concentration (Each Referenced on FL464)**

| peptide | PSD | this experiment |
|---|---|---|
| FL464 | 1.00 | 1.00 ± 0.2 |
| FL464 C1/A | 51.2 | 1.10 ± 0.13 |
| FL464 C2/A | 3.36 | 2.06 ± 0.08 |
| FL464 L/A | 0.51 | 3.07 ± 0.22 |
| FL464 P/A | 3.97 | 3.93 ± 0.03 |
| FL464 Q/A | 4.18 | |
| FL464 R/A | 14.9 | |
| FL464 S/A | 4.28 | |
| FL464 Y/A | 5.08 | |

PSD assays are a powerful and rather fast method for screening large quantities of phages, and thus peptides. Yet there are numerous factors that influence the outcome of a PSD assay. It is therefore essential to test the binding ability of the purified peptides again without phages to eliminate possible artifacts related to PSD.[11] As we are now able to prove that the priorly identified peptides bind LAP particles, the reasons why there are general problems in proving the interaction of PSD-derived chemically synthesized peptides are diverse and worth discussing. The reasons for this can be numerous. The results of PSD and this set of experiments, for example, are not directly comparable due to the completely different settings. This is due to the transition from a biological system to a more synthetic but also more application near system. While both the phages and the LAP particles are mobile during the PSD, in this experiment, the peptides are immobilized on a surface and only the target particles are mobile but settling fast. This inherits the disadvantage of a less dense packaging on the surface due to the blocking of binding sites by the relatively large particles compared to the small peptides. Furthermore, while proline and leucine hindered interactions in this experiment, they might help to shape the protein surface of the phage. This protein surface also can contribute to binding affinities, either by reducing the binding


https://doi.org/10.1021/acsomega.1c04343
ACS Omega 2022, 7, 187−197

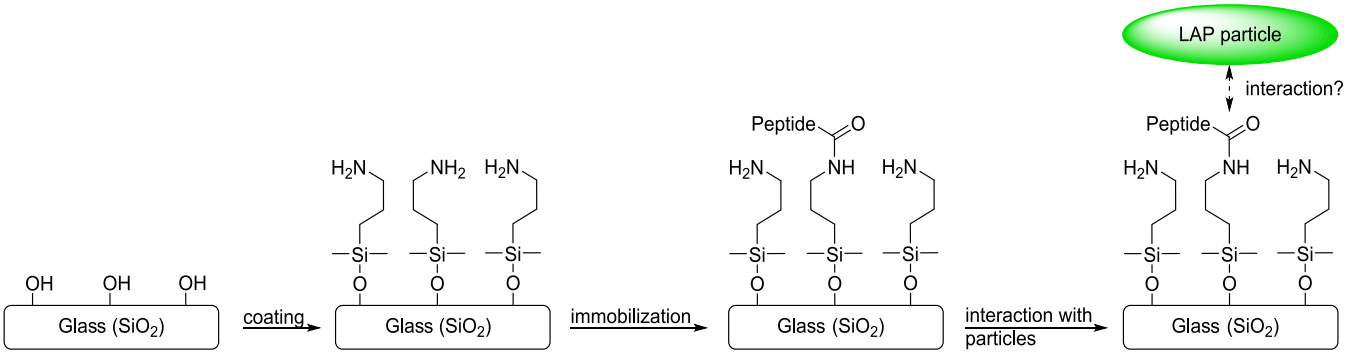


**Figure 10.** Overall scheme of the steps for the preparation of the glass substrates and binding studies of the immobilized peptides. Step 1: Coating the glass surface with APDMES; Step 2: Immobilization of the peptide via C-terminus; Step 3: Carrying out peptide−particle interaction studies.

affinity due to unfavorable interactions with the particles or vice versa. Furthermore, the protein itself has an effect on the structure of the peptide itself. Another unknown factor during PSD is a posttranslational modification by the bacteria during the amplification of the phages, which adds some uncertainties that are hard or impractical to control.[12] In addition, there can be tremendous differences during the amplification step with some phages being amplified significantly more often than others and thus distorting the results of the PSD. In general, another factor that needs to be considered is the amount of peptide itself. While the interaction of a single peptide molecule might not be strong, the phage surface displays the used PVIII protein up to 4000 times.[13−15] Although the percentage of the expressed fusion protein varies in a range between 10 and 40%, this would account for a number of at least 400 peptides displayed on the surface while also varying depending on the sequence.[16,17] In addition, while the binding of a single peptide molecule might be weak, the phage in contrast can act as a kind of chelator for the particles and strengthen the overall binding due to its multiple binding spots. Another factor to keep in mind is the changed net charge of the free peptide. The peptides are bound to the phage via the C-terminus of the peptide. Transitioning toward free peptides, this C-terminus bears a carboxylic functionality and therefore adds a possible negative charge but also enabling carboxylic acid chemistry to happen. A common method to prevent this issue is amidating the C-terminus during the synthesis of the peptide. However, also amidating a carboxylic acid results in a change of electron density and it changes also the proton acceptor/donor properties of this group as well, which can influence possible interactions.

One of the most commonly used methods for the separation of minerals and ores is froth flotation. In the froth flotation of rare earth minerals, typical dosages of collectors range from 500 g/t (e.g., of an ionic liquid) up to 1500 g/t (e.g., of sodium oleate) were reported previously.[18,19] For the separation of lamp powders, including LAP, by flotation, Hirajima et al. reported dosages of up to 3000 g/t for the usage of sodium oleate.[20] These obtained dosages are however highly specific for the used separation process and can change drastically depending on the process, the minerals, and the complexity of the separation process investigated. With the measured and calculated amount of peptide immobilized, and assumed it is similar in both experiments, one can calculate a needed dosage of immobilized peptide per ton of LAP. These range from ∼12 kg/t for FL464 to around 500−700 g/t for the peptides FL464 P/A and FL464 L/A. Although these numbers need to be taken carefully and might not reflect the dosage needed in future real application processes, these estimated low dosages show the high potential of immobilized peptides for the development of future separation processes. Furthermore, the peptides showed selective behavior against LAP compared to the other CESL-contained phosphors YOX and BAM. The high unspecific binding of YOX can be overcome with the use of already existing recycling techniques selective for YOX.[5] In that case, the use of peptide-based carriers could eventually lead to recycling techniques highly selective for LAP. However, one must keep in mind that the commonly used collectors, such as oleate or diesel, are rather inexpensive while peptides are in general more expensive. This burden of high initial investment could be overcome using immobilized peptides once a reusable carrier is developed. This also has the potential to reduce waste and to save precious resources, rendering peptides as a potentially greener and more sustainable alternative.

## 4. CONCLUSIONS

Working with PSD-derived peptides often proves challenging due to the changed systematic approaches. Going from a mobile carrier with multiple potential binding spots to a system with only one binding spot in solution inherits clear disadvantages. A phage mimicking approach by site-selective immobilization of RCQYPLCS (FL464) and its alanine-screening derivatives on modified glass supports was introduced to overcome those problems. We were able to state a proof of principle on peptide-modified surfaces that show adhesive properties against the fluorescent powder LAP. In our case, RCQYPACS (FL464 L/A) and RCQYAPCS (FL464 P/A) showed overall the most adhesion in our experiments with 3 and up to 4 times more LAP bound than FL464. The results of this study differ to some extent from the results of the PSD, underlining the troublesome transition from PSD to more realistic applications.[6] The aforementioned method showed reliable results with good flexibility. The method is equally suitable for fast screenings on commercially available microscopic slides as well as quantitative measurements for the investigation of various factors like concentration dependencies or the evaluation of elution conditions. Furthermore, we were able to calculate the amount of LAP bound on the peptides and were able to measure the amount of peptides immobilized, enabling us to estimate dosages of around 500 g/t for the peptides used for this particular setup. This is more than 5 times less amount compared to other collector dosages used in REE flotation, which shows the


https://doi.org/10.1021/acsomega.1c04343
ACS Omega 2022, 7, 187−197

Table 6. Overview of the Used Peptides, Their Amino Acid Sequences, and Their Molar Mass

| alias | peptide sequence[a] | $M$ [g·mol$^{-1}$] | alias | peptide sequence[a] | $M$ [g·mol$^{-1}$] |
|---|---|---|---|---|---|
| FL464 | RCQYPLCS-OH | 967.13 | FL464 Q/A | RCAYPLCS-OH | 910.08 |
| FL464 C1+C2/A | RAQYPLAS-OH | 905.02 | FL464 R/A | ACQYPLCS-OH | 882.02 |
| FL464 C1/A | RAQYPLCS-OH | 937.08 | FL464 S/A | RCQYPLCA-OH | 951.13 |
| FL464 C2/A | RCQYPLAS-OH | 937.08 | FL464 Y/A | RCQAPLCS-OH | 875.03 |
| FL464 L/A | RCQYPACS-OH | 925.05 | FL606 | TSTQCPSHIRAC LKKR-OH | 1827.16 |
| FL464 P/A | RCQYALCS-OH | 941.09 | | | |

[a]Bold marked **C** are forming a cysteine bridge.

potential of immobilized peptides for separation processes, especially once they are immobilized on reusable carriers.

Overall, the used phage mimicking approach offers a new set of convenient experiments for scientists working with PSD and the interaction toward particles and broadens the analytical repertoire. In general, phage mimicking approaches seem promising for conceptual new applications of PSD-derived knowledge. Reusable phage mimicking peptide carriers could lower the cost for industrial processes, thus helping in the introduction of novel bio-inspired recycling techniques.

## 5. MATERIALS AND METHODS

**5.1. Conception of the Experiment.** For comparison, proof and evaluation of peptide−particle−interactions peptides were immobilized on glass supports. 3-Aminopropylethoxy-(dimethyl)silane (APDMES) was chosen as a coating for further enabling immobilization of the peptides. APDMES introduces reactive amino groups onto the glass surface that are suitable for the immobilization of the peptides. The coupling onto the amine-functionalized glass was done via active ester-mediated coupling using benzotriazole-1-yl-oxy-tripyrrolidinophosphonium-hexafluorophosphate (PyBOP) as an activator for the carboxylic acid at the C-terminus of the peptide and diisopropylethylamine (DiPEA) is used as a base. In our case, the chosen immobilization route is selective for the free C-terminus of the peptide, enabling mimicking of the phage surface. The scheme of the overall process is shown in Figure 10. In each experiment, triplicates were used. The peptides used, their sequences, and molar masses are listed in Table 6.

**5.2. Chemicals and Supplier.** All of the chemicals used are commercially available with a minimum grade of "for synthesis". 3-Aminopropylethoxy(dimethyl)silane (APDMES; CAS−Nr 18306-79-1; purity 97%) was obtained from abcr GmbH, Germany. Benzotriazole-1-yl-oxytripyrrolidinophosphonium-hexafluorophosphate (PyBOP; CAS−Nr 128625-52-5; purity ≥98.5%) and diisopropylethylamine (DiPEA; CAS−Nr 7087-68-5; purity ≥99%) were obtained from Carl Roth GmbH + Co. KG, Germany. Tetrahydrofuran (THF; CAS−Nr 109-99-9; purity ≥99.9%) was dried over a freshly activated molecular sieve (3 Å, CAS−Nr 1318-02-1). Both were obtained from Sigma-Aldrich Chemie GmbH, Germany. The peptides were synthesized by DGpeptides, Co., Ltd., Hangzhou City, China (TFA salt, purity >95%). The diagnostic microscopic slides were free samples from Waldemar Knittel Glasbearbeitungs GmbH, Germany. The microscopic slides (Brand: labsolute) were obtained from Th. Geyer GmbH & Co. KG, Germany. The glass-coated microplates (Brand: WebSeal Plate+, 8 × 12 array; flat bottom; diameter: 7 mm) were obtained from Thermo Fisher Scientific, Inc. $LaPO_4$:Ce,Tb (LAP), $Y_2O_3$:Eu (YOX), and $BaMgAl_{10}O_{17}$:Eu (BAM) were obtained from Leuchtstoffwerk Breitungen GmbH, Germany, with a mean diameter of 2 μm, determined with particle analysis via FIJI ImageJ (NIH, v. 1.5.3).

**5.3. Immobilization of Peptides on Commercial Diagnostic Slides.** On commercial diagnostic slides, 5 μL (approx. 77 nmol, 1.0 equiv) of the various peptides dissolved in NMP were pipetted. To a 37 mM (19 mg in 1 mL NMP) PyBOP solution, 11 μL of DiPEA was added. Afterward, 2.5 μL (92 nmol, 1.2 equiv PyBOP, 3.7 equiv DiPEA) of this coupling agent solution was pipetted to the peptides on the glass surface and mixed by pipetting 3 times. The slides were covered and let rest for 2 h before being washed with Milli-Q water.

**5.4. Binding Test on Commercial Diagnostic Slides.** A LAP suspension (5 μL; 30 mg/mL) was pipetted onto the diagnostic slides and incubated for 5 min. Afterward, the slides were dipped and shaken three times each in three beakers with Milli-Q water to wash off loosely bound LAP.

**5.5. Amine Functionalization of Glass-Coated MTPs.** The MTPs were used as delivered and without further cleaning. A solution of APDMES in dry THF (100 μL; 0.5 vol %) was pipetted into the wells. The well plate was covered and washed three times with Milli-Q water after 30 min and dried overnight at 70 °C.

**5.6. Peptide Immobilization on Amine-Functionalized Glass-Coated MTPs for Fast Sequence Screening.** To the APDMES-functionalized MTP, 5 μL of the respective peptides (20 mg/mL; approx. 83 nmol, 1 equiv) in NMP was pipetted into the wells as triplicates. A coupling agent solution containing 7 mM PyBOP and 18 mM DiPEA was prepared freshly. From this solution, 13 μL was added to each well (PyBOP: 100 nmol, 1.2 equiv; DiPEA: 250 nmol, 3.0 equiv) and diluted with 87 μL of NMP. The plate was covered and shaken on a horizontal shaker at room temperature for 2 h. The solvent was removed, and the plate was washed three times with Milli-Q water.

**5.7. Immobilizing Peptides on Amine-Functionalized Glass-Coated MTPs for Concentration Screening.** An APDMES-functionalized MTP was used. Three rows, that later were used for the calibration curve, were covered to prevent contamination; see Section 5.9. Three different concentrations of freshly prepared peptide solutions were used in triplicates with the amount of substance containing 48, 95, and 143 nmol, respectively. To each well, varied amounts of 86.0, 72.1, and 58.2 μL NMP were added to later achieve an overall volume of approx. 100 μL. The amount of peptide was pipetted into the wells. Finally, varied amounts of solution of 12.1, 24.2, and 36.3 μL of a coupling agent solution containing 4 mM PyBOP and 11 mM DiPEA in NMP were added. This is corresponding to 1 equiv for PyBOP and 3 equiv for DiPEA. The overall concentrations in 100 μL NMP are listed in Table 7. The plate was covered and shaken on a horizontal shaker at room


https://doi.org/10.1021/acsomega.1c04343
ACS Omega 2022, 7, 187−197

temperature for 3 h. The solvent was removed, and the plate was washed three times with Milli-Q water.

**Table 7. Used Concentrations of the Reagents for the Immobilization for the Concentration Screening Experiment**

| amount of substance used [nmol] | concentration peptide [mM] | concentration PyBOP [mM] | concentration DiPEA [mM] |
|---|---|---|---|
| 48 | 0.48 | 0.48 | 1.44 |
| 96 | 0.96 | 0.96 | 2.88 |
| 143 | 1.43 | 1.43 | 4.32 |

**5.8. Particle Binding Test.** A suspension of LAP (30 mg/mL) was added onto the modified substrates. For microscopic slides and MTPs, 10 and 110 $\mu$L were used, respectively. After 5 min of incubation, the samples were washed once with Milli-Q water, except the concentration screening (Section 5.7) where the plates were washed three times.

**5.9. Calibration Curve.** After the particle binding test (see Section 5.8), the cover of the APDMES-functionalized MTP plate (see Section 5.7) was removed. A 1.0 mg/mL suspension of LAP was used. An overall volume of 100 $\mu$L was used, and Milli-Q water was laid upfront. Afterward, the LAP suspension was vortexed for 3 s for each pipetting step and the amount of LAP was transferred into the wells and pipetted up and down three times each to ensure proper distribution. For the calibration curve, eight steps were used: 0 $\mu$g—20 $\mu$g—40 $\mu$g—50 $\mu$g—60 $\mu$g—70 $\mu$g—80 $\mu$g—100 $\mu$g. The plate was left for 2 days at room temperature to evaporate slowly.

**5.10. Fluorescence Scanning.** Fluorescence scanning was performed using a Mithras$^2$ LB 943 (Fa. Berthold Technologies GmbH & Co. KG) and software MikroWin 2013 version 5.53. The lamp energy was set to 40% with a fixed excitation wavelength of 365 nm and a fixed emission wavelength of 545 nm. As scanning parameters, round wells with 20 × 20 scans and a point displacement of 0.45 mm were chosen with a scanning time per pixel of 0.1 s. For quantification, the fluorescence signal on every point was summed and the mean of the triplicates as well as the relative standard error of the mean (REM) were calculated. The calculated data as well as the fluorescence sums are available in Tables S2−S5.

As the background fluorescence is changing as particles are bound on top of the surface, no additional correction is used. Instead, a calibration curve was used to enable quantification and to compensate for the background fluorescence.

For the test of significance, two-tailed two-sample *t*-tests were performed. Graphs in figures were marked as significant with rounded *P* values ≤.05, and the *P* values are given in the caption and/or corresponding table.

The raw data obtained are available via HZDR RODARE, and the processed data are shown in the Supporting Information.[21]

**5.11. Measurement of Immobilized Peptides.** An APDMES-functionalized MTP was used. In triplicates, peptide concentrations of 0.05, 0.48, 0.96, and 1.43 mM were used and immobilized with corresponding 1 equiv PyBOP, 3 equiv DiPEA, and the lacking volume to 100 $\mu$L filled with NMP before adding of the reagents.

After immobilization of the peptides, the plate was dried at 70 °C overnight. UV−vis spectroscopy was performed using a Mithras$^2$ LB 943 (Fa. Berthold Technologies GmbH & Co. KG) and the software MikroWin 2013 version 5.53 via spectral scanning with 10 nm step size and 5 s measurement time per step. For quantification, the adsorption at 280 nm wavelength was used and a monolayer with 2 nm thickness was assumed. The extinction coefficient was determined from triplicates of peptide solutions containing 0.192 mM of the respective peptide dissolved in NMP and blanked against Milli-Q water containing 0.8% NMP, performed on a Specord 50 (Fa. Analytic Jena) with PMMA single-use cuvettes. The extinction coefficient of APDMES was determined from triplicates of 10 mM APDMES in water and blanked against Milli-Q water, performed on a Specord 50 with PMMA single-use cuvettes.

**5.12. Molecular Mechanic Energy Minimization Calculations.** Energy minimization calculations were performed using Chem3D Pro (v. 18.0.0.231). An MM2 forcefield was chosen, and minimization was performed until an RMS Gradient of 0.01 was reached.

**5.13. Selectivity Test.** Two APDMES-functionalized MTP were used. One plate contained the binding experiments, while the other plate was used to obtain the calibration curves.

For the immobilization of peptides, the peptide solution was used in triplicate with the amount of substance containing 95 nmol. To each well, 72 $\mu$L of NMP was added to later achieve an overall volume of approx. 100 $\mu$L. The amount of peptide was pipetted into the wells. Finally, 24.2 $\mu$L of a coupling agent solution containing 4 mM PyBOP and 11 mM DiPEA in NMP was added. This is corresponding to 1 equiv for PyBOP and 3 equiv for DiPEA. The plate was covered and shaken on a horizontal shaker at room temperature for 2 h. The solvent was removed, and the plate was washed three times with Milli-Q water.

For the calibration curves, a 1.0 mg/mL suspension of LAP was used. An overall volume of 100 $\mu$L was used and Milli-Q water was laid upfront. Afterward, the LAP suspension was vortexed for 3 s for each pipetting step and the amount of LAP was transferred into the wells and pipetted up and down three times each to ensure proper distribution. For the calibration curve, eight steps were used: 0 $\mu$g—20 $\mu$g—40 $\mu$g—50 $\mu$g—60 $\mu$g—70 $\mu$g—80 $\mu$g—100 $\mu$g. The plate was dried for 5 h at 80 °C. The used calibration curves are included in the Supporting Information.

## ■ ASSOCIATED CONTENT

### Supporting Information

The Supporting Information is available free of charge at https://pubs.acs.org/doi/10.1021/acsomega.1c04343.

Pipetting scheme of the fast semiquantitative screening for peptides (Table S1); fluorescence sums of the fast semiquantitative screening for peptides (Table S2); results of the semiquantitative screening for peptides (Table S3); results of UV−vis absorbance measurements (Table S4); results of UV−vis absorbance measurements of 0.192 mM peptide solution, blanked against Milli-Q water with 0.8% NMP and calculated extinction coefficients (Table S5); image of the molecule structures after MM2 energy minimization calculations (Figure S1); image of the comparison of spots after immobilization of peptide on microscopic slides (Figure S2); functionalizing of microscopic slides with APDMES (Method 5.13); immobilization of peptide on functionalized microscopic slides (Method 5.14); results of



https://doi.org/10.1021/acsomega.1c04343
ACS Omega 2022, 7, 187−197

pretests on microscopic slides (Result 2.6); calibration curves for YOX and BAM (Figure S3); results and used data for calibration curves for YOX and BAM (Table S6); and results of the binding experiments for YOX and BAM (Table S7) (PDF)

## AUTHOR INFORMATION


### Corresponding Author

**Martin Schrader** − *Department of Biotechnology, Helmholtz Institute Freiberg for Resource Technology, Helmholtz Center Dresden-Rossendorf, 01328 Dresden, Germany;* orcid.org/0000-0001-6855-8068; Email: m.schrader@hzdr.de

### Authors

**Caroline Bobeth** − *Department of Biotechnology, Helmholtz Institute Freiberg for Resource Technology, Helmholtz Center Dresden-Rossendorf, 01328 Dresden, Germany*

**Franziska L. Lederer** − *Department of Biotechnology, Helmholtz Institute Freiberg for Resource Technology, Helmholtz Center Dresden-Rossendorf, 01328 Dresden, Germany*

Complete contact information is available at: https://pubs.acs.org/10.1021/acsomega.1c04343


### Author Contributions

M.S. contributed to conceptualization. M.S. and C.B. performed methodology. M.S. contributed to validation, formal analysis, investigation, data curation, visualization, and writing—original draft preparation. Writing—review and editing was performed by M.S., F.L.L., and C.B. F.L.L. performed supervision, project administration, and funding acquisition. All authors have read and approved the published version of the manuscript.

### Notes

The authors declare no competing financial interest.

## ACKNOWLEDGMENTS

The authors thank Waldemar Knittel Glasbearbeitungs GmbH for providing free samples of their diagnostic slides.

## REFERENCES


(1) Ciacci, L.; Reck, B. K.; Nassar, N. T.; Graedel, T. E. Lost by Design. *Environ. Sci. Technol.* **2015**, *49*, 9443−9451.

(2) Swain, N.; Mishra, S. A review on the recovery and separation of rare earths and transition metals from secondary resources. *J. Cleaner Prod.* **2019**, *220*, 884−898.

(3) Binnemans, K.; Jones, P. T. Perspectives for the recovery of rare earths from end-of-life fluorescent lamps. *J. Rare Earths* **2014**, *32*, 195−200.

(4) Binnemans, K.; Jones, P. T.; Blanpain, B.; Van Gerven, T.; Yang, Y. X.; Walton, A.; Buchert, M. , Recycling of rare earths: a critical review. *J. Cleaner Prod.* **2013**, *51*, 1−22.

(5) Dupont, D.; Binnemans, K. Rare-earth recycling using a functionalized ionic liquid for the selective dissolution and revalorization of Y2O3:Eu3+ from lamp phosphor waste. *Green Chem.* **2015**, *17*, 856−868.

(6) Lederer, F. L.; Curtis, S. B.; Bachmann, S.; Dunbar, W. S.; MacGillivray, R. T. Identification of lanthanum-specific peptides for future recycling of rare earth elements from compact fluorescent lamps. *Biotechnol. Bioeng.* **2017**, *114*, 1016−1024.

(7) Braun, R.; Bachmann, S.; Schonberger, N.; Matys, S.; Lederer, F.; Pollmann, K. Peptides as biosorbents - Promising tools for resource recovery. *Res. Microbiol.* **2018**, *169*, 649−658.

(8) Curtis, S.; Lederer, F. L.; Dunbar, W. S.; MacGillivray, R. T. Identification of mineral-binding peptides that discriminate between chalcopyrite and enargite. *Biotechnol. Bioeng.* **2017**, *114*, 998−1005.

(9) Pollmann, K.; Kutschke, S.; Matys, S.; Raff, J.; Hlawacek, G.; Lederer, F. L. Bio-recycling of metals: Recycling of technical products using biological applications. *Biotechnol. Adv.* **2018**, *36*, 1048−1062.

(10) Yadav, A. R.; Sriram, R.; Carter, J. A.; Miller, B. L. Comparative study of solution−phase and vapor−phase deposition of aminosilanes on silicon dioxide surfaces. *Mater. Sci. Eng. C* **2014**, *35*, 283−290.

(11) Tim Clackson, H. B. L. *Phage Display: A Practical Approach*, 1st ed.; Oxford University Press: Oxford, U.K., 2004.

(12) Macek, B.; Forchhammer, K.; Hardouin, J.; Weber-Ban, E.; Grangeasse, C.; Mijakovic, I. Protein post-translational modifications in bacteria. *Nat. Rev. Microbiol.* **2019**, *17*, 651−664.

(13) Bonnycastle, L. L.; Mehroke, J. S.; Rashed, M.; Gong, X.; Scott, J. K. Probing the basis of antibody reactivity with a panel of constrained peptide libraries displayed by filamentous phage. *J. Mol. Biol.* **1996**, *258*, 747−762.

(14) Smith, G. P.; Petrenko, V. A. Phage Display. *Chem. Rev.* **1997**, *97*, 391−410.

(15) Newman, J.; Swinney, H. L.; Day, L. A. Hydrodynamic properties and structure of fd virus. *J. Mol. Biol.* **1977**, *116*, 593−603.

(16) Malik, P.; Terry, T. D.; Gowda, L. R.; Langara, A.; Petukhov, S. A.; Symmons, M. F.; Welsh, L. C.; Marvin, D. A.; Perham, R. N. Role of Capsid Structure and Membrane Protein Processing in Determining the Size and Copy Number of Peptides Displayed on the Major Coat Protein of Filamentous Bacteriophage. *J. Mol. Biol.* **1996**, *260*, 9−21.

(17) Hess, G. T.; Cragnolini, J. J.; Popp, M. W.; Allen, M. A.; Dougan, S. K.; Spooner, E.; Ploegh, H. L.; Belcher, A. M.; Guimaraes, C. P. M13 bacteriophage display framework that allows sortase-mediated modification of surface-accessible phage proteins. *Bioconjugate Chem.* **2012**, *23*, 1478−1487.

(18) Li, R.; Marion, C.; Espiritu, E. R. L.; Multani, R.; Sun, X.; Waters, K. E. Investigating the use of an ionic liquid for rare earth mineral flotation. *J. Rare Earths* **2021**, *39*, 866−874.

(19) Zhang, W.; Honaker, R.; Groppo, J. Concentration of rare earth minerals from coal by froth flotation. *Miner. Metall. Process.* **2017**, *34*, 132−137.

(20) Hirajima, T.; Bissombolo, A.; Sasaki, K.; Nakayama, K.; Hirai, H.; Tsunekawa, M. Floatability of rare earth phosphors from waste fluorescent lamps. *Int. J. Miner. Process.* **2005**, *77*, 187−198.

(21) Schrader, M. Raw data: "Quantification of Peptide-Bound Particles: A Phage Mimicking Approach via Site-Selective Immobilization on Glass". 2021, DOI: 10.14278/rodare.1192.